

Evaluating the Accuracy of Wind Turbine Power-Speed Characteristics Fits for the Generator Control Region

Al-Motasem I. Aldaoudeyeh*[‡] and Khaled Alzaareer**

*Tafila Technical University, Tafila, Jordan

**University of Quebec, Montreal-Quebec, Canada

(almotasem.aldaoudeye@ndsu.edu, kaledz87@yahoo.com)

[‡] Corresponding Author; Al-Motasem I. Aldaoudeyeh Tafila Technical University, Tafila, Jordan;
almotasem.aldaoudeye@ndsu.edu

Received: 18.05.2020 Accepted: 15.06.2020

Abstract- The generator control region in wind turbines is generally hard to represent mathematically. This paper evaluates the accuracy of wind turbine fits for such a region, namely the polynomial, the approximate cubic, and the exponential fits. The study demonstrates how higher-order polynomials are not necessarily more accurate than lower-order ones. Three different wind turbines are modeled, and calculations of the capacity factor and the average produced power are carried out to examine the modeling limitations of the approximate cubic and the exponential fits. Results show that the exponential fit has low accuracy for low wind speeds, especially when the wind turbine curve is ‘S-shaped’ in the generator control region. The approximate cubic fit is also shown to always over-estimate the annual energy yield of wind turbines.

Keywords: wind turbine characteristics; curve fitting; Weibull distribution; capacity factor; energy yield.

Nomenclature

AEP	Annual Energy Production	RMSE	Root Mean Square Error
AF	Availability Factor	SCADA	Supervisory Control and Data Acquisition
ANN	Artificial Neural Networks	WT	Wind Turbine
CF	Capacity Factor	WTPSC	Wind Turbine Power Speed Characteristics
GCR	Generator Control Region		
GP-ANN	Gaussian Processes Artificial Neural Networks		
MC	Monte Carlo		
MSE	Mean Square Error		
PDF	Probability Density Function		

1. Introduction

The global installed capacity of WTs has grown from 100GW in 2008 to 542GW in 2018. Furthermore, it is projected that such a figure would reach 1787GW in 2030 [1]. Challenges, however, are still present regarding increasing WTs efficiency (especially at low wind speeds), integration of large wind farms into bulk power grids (e.g., stability), risk assessment, and modeling of wind turbines and wind regimes. Efforts are made in the literature to overcome many of these

issues (as in [2]), and this paper focuses on the accuracy of different wind turbine power-speed characteristics fits and their impact on their predictions of energy yield.

Ref. [3] devises a method to appropriately select WTs sites for given Weibull distribution parameters along with cut-in, cut-out, and rated speeds of WTs. The authors derive CF and the AF (i.e., the probability that a WT will remain connected to the grid during an entire year) in terms of Weibull distribution parameters as well as some specifications of the WTs (e.g., cut-in speed). They then compare the suitability of sites depending on the magnitude of CF, where the site-WT combination of a higher capacity factor is classified as a better alternative. When, however, the CFs of multiple site-WT combinations match each other, the priority goes to the combinations that provide higher AFs.

Ref. [4] statistically analyzes the wind energy potential in Hong Kong using Weibull distribution. The operating probability of WTs is found in terms of its ratings and Weibull distribution parameters for the sites of interest (similar to [2]). The seasonal variation of the most probable wind speeds and Weibull distribution parameters are used as a basis of analysis and decision making. The authors conclude that the cut-in speed has a significant effect on the WT operation probability.

Authors of [5] assess the suitability of five different candidate sites for wind power projects in Jordan. The study uses the power density in certain areas as a major criterion in the selection of the site. They report that seasonal variations as a key factor that strongly influences decision making.

Combining sensitivity study and MC method to understand the effects of uncertainty in WT projects is devised in Ref. [6]. The authors classify wind speed, electricity tariffs, installation costs, and the power curve of WT as key factors that influence a wind farm performance. They, however, exclude air density as it does not vary a lot throughout the year.

Ref. [7] studies modeling the power of retrofitted WTs using ANN. Authors argue that WTs are subjected to non-stationary conditions, meaning that comparing energy production before and after upgrades is not a suitable way to compare the improvement due to the upgrade. Thus, they use ANN with a data-driven approach. This is done by sampling 10-minute data for wind power. The authors devise that to improve power for a given upgrade, we must apply the following 1) optimize the pitch angle control of the blade; 2) apply “blade retrofitting”, and 3) extend the power curve for very high wind speed.

Ref. [8] describes an automatic GP-ANN to approximate the wind power curve depending on a minimal group of input variables, which is wind speed and wind direction. They then compare the estimated AEP with the actually produced one. Furthermore, the authors compare their work with different parametric and non-parametric power curves.

Ref. [9] proposes a probabilistic model of WTPSC, which are established using fuzzy clustering, ANN, as well as MC. The authors use SCADA data from Chinese wind farms to compare their methods with deterministic ones. Further, they

recommend that probabilistic WTPSC be used for forecasting and health management of WTs.

To our knowledge, papers in the literature have the following drawbacks when evaluating the accuracy of WTPSC or devising new techniques 1) Despite using empirical data (such as [7]; [8]), they do not include different types of possible wind regimes (i.e., the studies are only for very specific regions), and 2) They do not address the accuracy of WTPSC, resulting in from positive errors (i.e., modeled WTPSC is above empirical data provided by the manufacturer) or negative errors (i.e., modeled WTPSC is below the empirical data provided by the manufacturer). In fact, even the most recent review papers WTPSC modeling ([10]–[12]) did not mention that any paper covers anything about the implications of such errors.

The contributions of this paper include the following

1. it is very well-known that wind speed probability distribution may vary depending on annual, seasonal, and monthly variations. Using realistic Weibull distribution data for wind regimes at different sites in the world as well as manufacturer-provided measurements for WTs, we show that some models may accurately predict the total energy yield over a year. However, predictions accuracy for a shorter duration that sometimes generally have low or high wind speeds (e.g., one month) may drop (Sections 3 and 4)

2. it corrects some misconceptions about the accuracy of WTPSC models. For instance, it is believed in the literature that the higher the order of polynomial fits, the better the fitting accuracy (SubSection 1.4)

3. it provides rigorous coverage of WTPSC regions (SubSection 1.2). Further, it explains the reason that WTPSC is not necessarily cubic despite the fact that power in the wind is proportional to the cube of wind speed (SubSection 1.4)

The paper is organized as follows: the rest of this section depicts different aspects of interest on WT characteristics and their mathematical representations. Section 2 defines Weibull distribution, the capacity factor, and the mean wind speed. Section 3 presents and discusses the numerical results of the WT mathematical fits. Section 4 concludes the paper.

1.1. Wind Energy Conversion

The available power in the wind can be expressed as [13]

$$P_w = \frac{1}{2} \rho A v_w^3 \quad (1)$$

The electrical power extracted by a Wind Turbine (WT) and injected into the grid is given in terms of wind speed (v_w) as follows [13]–[15]

$$P_{e, WT} = \frac{1}{2} \rho A v_w^3 C_{p, e}(\lambda, \beta) \quad (2)$$

$$= \frac{1}{2} \rho \pi R^2 v_w^3 C_{p, e}(\lambda, \beta) = P_w C_{p, e}(\lambda, \beta) \quad (3)$$

Where ρ is the air mass density (for a temperature of $15^\circ C$ and $1 atm$, a dry air has $\rho = 1.2250 kg/m^3$ [16]), R is the rotor radius, and P_w is the total power in the wind in

watts. v_w is the wind speed in m/s . $C_{p,e}$ is called the “effective” power coefficient (because it includes mechanical and electrical losses).

$C_{p,e}$ is a nonlinear function of the Tip Speed Ratio (λ) and the pitch angle of the blades (β). Readers interested in knowing about this relationship are advised to refer to [17]–[19]. It quantifies the fraction of the wind power that gets converted into electrical power. $C_{p,e}$ depends on the blade design and friction losses in the drivetrain as well as electrical losses in the generator and any power electronic interfaces between it and the transformers. Note that even though $C_{p,e}$ is sometimes called the aerodynamic coefficient, calling it this way might be misleading. This is because manufacturers provide electrical output characteristics as a function of wind speed. Thus, data provided by the manufacturer for power coefficient includes not only the losses in the blades as they convert wind power into mechanical power at the main shaft, but also mechanical and electrical losses in bearings, gearboxes, the generators, power electronic interfaces, etc. The effective power coefficient has a theoretical limit of 16/27 (Betz limit), but practically it is around 0.47 to for large WTs [20] and 0.35 for small WTs [21].

TSR has a strong influence on the efficiency of a WT, which is defined as the ratio of the tangential speed at the blade tip to the wind speed [22]; [23]

$$TSR = \lambda = \frac{\text{Blade Tip Speed}}{\text{Wind Speed}} = \frac{\omega R}{v_w} \quad (4)$$

Where ω is the angular speed of the blades. If the blades rotated slowly, they would spill too much of the wind power hence convert a small portion of it into a mechanical form. If blades rotated very quickly, they would cause turbulence in the wind, which significantly reduces the lift force on the blades and, consequently, the power extracted from the wind. Hence, to capture the maximum power at different wind speeds, the rotating speed of the WT must be adjusted according to the v_w [22]. The optimal TSR (λ_{opt}) is a function of blades number and shape. Thus, each WT would have its own (fixed) λ_{opt} . Optimal TSR is typically within the range of 6 to 9.

1.2. Wind Turbine Characteristics

A WTPSC curve is described by four operation regions (Fig. 1), which we divide by remarkable speeds of the wind that influence how the WT operates

➤ **Cut-in speed ($v_{ci} \sim 3$ to $4m/s$).** Below cut-in speed, the torque developed by the rotor is not sufficient to overcome the inertia and friction (e.g., bearing friction) in the drive-train to produce a net positive torque to be delivered to the generator [24]. Thus, the rotor is blocked by a mechanical brake, and the turbine is turned off. In fact, some studies even reported that inertia and friction were not overcome even when the wind speed is slightly above v_{ci} [25]. The region between v_{ci} and the rated wind speed is called the GCR, a region in which the control system maximizes the captured power by maintaining λ

at λ_{opt} . The angle of attack in GCR is set to its rated value, and there is no pitch or stall control actions

- **Rated speed ($v_r \sim 10$ to $15m/s$).** Beyond this speed (and up to the cut-out speed), the power output is limited through an aerodynamic power control in the blade, which keeps the electric power output constant at rated value [22]. In such a region, which is called Pitch/Stall Control Region, a part of the wind power is spilled hence both of the effective power coefficient and efficiency decrease
- **Cut-out speed ($v_{co} \sim 20$ to $25m/s$).** This speed is a safety constraint during WT operation. The WT shuts down at high wind speeds to prevent damage to itself. In practice, however, the WT is not turned off immediately, but only after a few minutes (e.g., 10 minutes) during which the average wind speed exceeds the specified cut-out speed. Even after such a period passes, the turbine output is ramped down gradually to zero. Such a measure is essential to maintain the stability of the electric grid

In addition to the speeds mentioned above, we also have the survival speed (~ 50 to $60m/s$) which is not shown in WTPSC curves, but usually provided by manufacturers. It is the maximum wind speed that the WT sustains and would be damaged if it was exposed to wind speeds above it.

Fig. 1 depicts the characteristic curve of a typical stall/pitch controlled WT. The same figure also shows the wind characteristics and the maximum theoretically usable power. It is important to note that the $P_{e,WT}$ in WTPSC is the electrical output of the wind turbine rather than the mechanical power at the shaft of the hub.

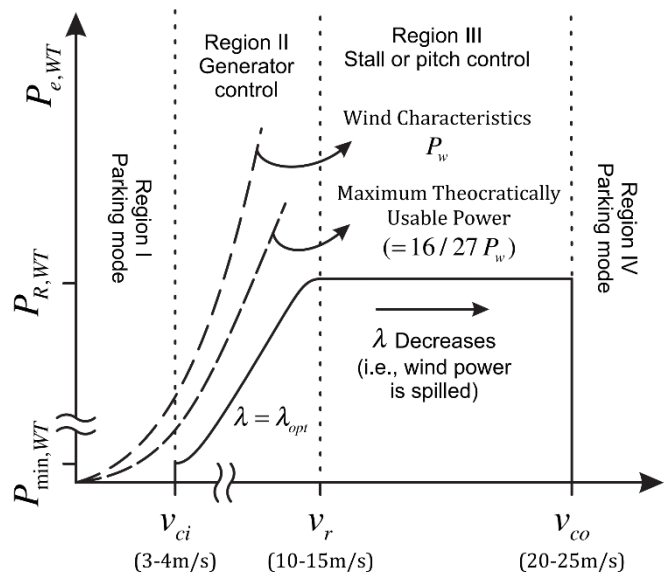


Fig. 1. WTPSC and its Different Operating Regions

1.3. Mathematical Representations of WTPSC Curves

Depending on the wind speed, a WT would

- turn off when $v_w < v_{ci}$ or $v_w > v_{co}$ meaning that in such regions $P_{e,WT} = 0$
- be controlled to extract the maximum power in the GCR (i.e., when $v_{ci} \leq v_w \leq v_r$) by making λ equal to λ_{opt} .

$C_{p,e}$ here varies due to different efficiencies of the blades, the gearbox, the generator, and the inverter at different wind speeds. The power output here is denoted as PGCR (v_w) and has different ways to model it as discussed in this section

- get its power output limited to its generator rating using stall/pitch control when $v_r \leq v_w \leq v_{co}$

The aforementioned is given mathematically as

$$P_{e,WT} = \begin{cases} 0 & v_w < v_{ci} \\ P_{GCR}(v_w) & v_{ci} \leq v_w \leq v_r \\ P_{R,WT} & v_r \leq v_w \leq v_{co} \\ 0 & v_w > v_{co} \end{cases} \quad (5)$$

$P_{R,WT}$ is the rated output power of the WT. $P_{GCR}(v_w)$ is handled with different mathematical representations that are intended to fit the mathematical expression with the manufacturer-provided data (i.e., empirical power-speed pairs in the GCR). In this paper, we examine three of them and enumerate them below [26] [27]

- n^{th} Degree Polynomial Fit where

$$P_{GCR}(v_w) = c_n v_w^n + c_{n-1} v_w^{n-1} + \dots + c_0 \quad (6)$$

where c_0, c_1, \dots, c_n are constants that are determined by curve fitting. The degree of the polynomial depends on the GCR curve. Ref. [28] suggests that a ninth-degree polynomial performs best. However, we see later in this paper how ninth-degree polynomial can sometimes perform worse than lower-order ones.

- Exponential Fit where

$$P_{GCR}(v_w) = \frac{1}{2} \rho \pi R^2 K_p (v_w^\beta - v_{ci}^\beta) \quad (7)$$

where K_p and β are constants determined by curve fitting.

- Approximate Cubic Fit where

$$P_{e,WT} = \frac{1}{2} \rho \pi R^2 v_w^3 C_{p,max} \quad (8)$$

where $C_{p,max}$ is the maximum value of the “effective” power coefficient where the term “effective” refers to including both mechanical and electrical losses [27]. It is worth noting that $C_{p,max}$ is not Betz coefficient nor is it equal to $C_{p,e}$ at v_r . $C_{p,max}$ might be either obtained directly from the manufacturer datasheet or calculated by finding the maximum value of $C_{p,e}$ using Eq. (3) for all power-speed pairs that the manufacturer provides for the GCR.

Finally, it is worth mentioning that such performance characteristics are only valid under normal operating conditions. When the WT operates under abnormal conditions, the characteristics could be different from the ones given in Eq. (6) [29].

1.4. The Degree of the Polynomial Fit and Its Accuracy

The fact that power in the wind exhibits cubic variation with wind speed means that the WTPSC in the GCR might be represented using a polynomial. However, the actual power extracted from the wind (i.e., $P_{e,WT}$) in the GCR does not necessarily resemble the cubic characteristics of the wind due to efficiency restrictions. In particular, the mechanical losses (e.g., gearbox or bearing and windage losses) and electrical losses (e.g., inverter losses) vary with wind speed. Consequently, different designs would result in different shapes of WTPSC in the GCR, which renders modeling such region troublesome and makes its mathematical representation a topic worth investigating. According to the reasons just mentioned, we cannot always use a cubic relationship and may need to use higher-order polynomials to get a better fit with the manufacturer-provided data. Counter-intuitively, a higher-order polynomial may not always be better. An example of such a case is shown in Fig. 2, with 9th, 8th, and 7th degrees polynomials used to fit the GCR in a 275kW WT.

Inaccuracies tend to occur at the lowest speeds. Near v_{ci} , the 9th order polynomial is not a good model as it predicts a decrease in power as the wind speed increases. Decreasing the order to 8 does not help and causes further inaccuracy (in fact, $P_{e,WT}$). However, the 7th order polynomial has better accuracy as it matches the power-speed pairs as given by the manufacturer but does not exhibit an inverse proportionality between power and speed near the v_{ci} . Thus, the main difference between the characteristics of higher order and lower order polynomials is that higher order polynomials may exhibit anomalies in their power predictions, while lowering the order of polynomials usually fixes this by producing monotonic relationship between wind speed and electrical power output predictions.

2. Calculating the Energy Yield and Capacity Factors of Wind Turbines

This section discusses three main topics of interest 1) Weibull probability distribution and typical values of its parameters; 2) calculation of the mean produced power using WTPSC and Weibull distribution, and 3) the capacity factor and some of its typical values. We use the mathematical calculations covered here in Section 3.

2.1. Weibull Distribution

Wind speeds in a specific location vary from time to time. Even small variations in wind speeds may result in large amounts of output power changes because the power available in the wind is proportional to the cube of wind speed. The Weibull distribution is commonly used to describe the PDF of wind regime over a long period (typically a year) and is given as [30]

$$f(v_w) = \frac{k}{c} \left(\frac{v_w}{c}\right)^{(k-1)} \exp\left[-\left(\frac{v_w}{c}\right)^k\right] \quad (9)$$

where $f(v_w)$ is the probability density of the wind speed, k (unitless) is the shape parameter, and c (m/s) is the scale

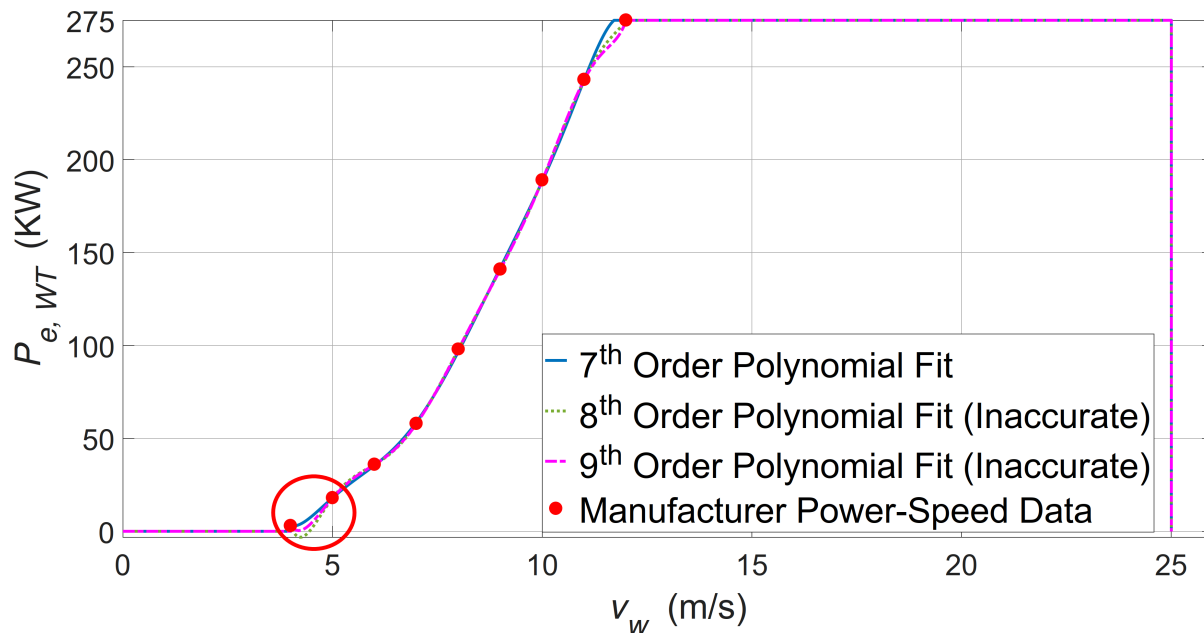


Fig. 2. International journal of renewable energy research

parameter. k is dimensionless parameter and characterizes the shape of the frequency distribution (hence, it is called the “shape” parameter) [31]. c quantifies the abundance of wind

on the site or how “windy” it is. If this parameter is large, then the average wind speed is high [13]. In most parts of the world, k is around 1.2 to 2.75 [32]. A high k (i.e., 2.5 to 3 [33]) results in a peaked distribution of wind speeds, which means that the site has a stable wind regime. A small k (1.2 to 1.5 [33]) results in a relatively flat distribution, which means we have a greater variation of wind speed around its annual mean. Both k and c need to be high in a favorable site. Thus, k and c provide engineers with an insight into the suitability of a candidate location for a WT farm project.

It is worth noting that wind is usually measured at lower heights, while the actual wind turbines are installed at higher hub heights than what is measured. However, when converting from wind speed to the other, the wind speed regime at higher hub height is still described using a Weibull distribution [34]. Furthermore, most recent papers on WTPSC modeling did not conclude that conversion of wind speeds affects the accuracy of WTPSC modeling [10]. However, an extrapolation might be needed during actual feasibility studies [35], when we finally want to choose the optimal size of wind turbines. Since this paper focuses on WTPSC curves while wind speed is still described by Weibull distribution regardless of the hub height, then we directly use typical Weibull distribution parameters (without extrapolation).

2.2. Mean Produced Power and Energy Yield

The mean produced power of a WT ($\bar{P}_{e,WT}$) in a given site is found by integrating the product of the WTPSC curve and the PDF of wind regime of the considered site over all possible wind speeds or [30]

$$\bar{P}_{e,WT} = \int_0^{\infty} P_{e,WT} f(v_w) dv_w \quad (10)$$

Note that the mean produced power corresponding to a certain speed range (from $v_{w,1}$ to $v_{w,2}$) can also be calculated by adjusting the boundaries of Eq. (10) as follows

$$\bar{P}_{e,WT}(v_{w,1}, v_{w,2}) = \int_{v_{w,1}}^{v_{w,2}} P_{e,WT} f(v_w) dv_w \quad (11)$$

The total energy production of a WT over a year is called the annual energy yield of that WT (E_{tot}). We can calculate it by multiplying $\bar{P}_{e,WT}$ by the number of hours in a year (= $365 \times 24 = 8760$) [36]

$$E_{tot} = 8760 \bar{P}_{e,WT} = 8760 \int_0^{\infty} P_{e,WT} f(v_w) dv_w \quad (12)$$

2.3. The Capacity Factor

The Capacity Factor (C_f) is the total amount of energy delivered over a period (typically a year) divided by the energy that could have been delivered if the WT operated at its full capacity over that period ($E_{R,tot}$). For a year, C_f is calculated as follows

$$C_f = \frac{E_{tot}}{E_{R,tot}} = \frac{E_{tot}}{8760 P_{R,WT}} \quad (13)$$

A typical range of C_f for on-shore wind farms is 0.25 to 0.40 [37]. For off-shore wind farms, the range is 0.35 to 0.50 [38]. However, a review conducted by NREL for different large-scale projects reports that C_f for wind farms can vary within a range of 0.25 to 0.50 for on-shore projects and 0.30 to 0.50 for off-shore projects, with the latter having a capacity-weighted average of 0.38 [38].

Table 1. Specifications of the Studied WTs

	GEV MP R	G58-850	E-92
Manufacturer	Vergnet	Vestas	Enercon
$P_{R, WT}$ (kW)	275	850	2350
v_{ci}	3.5	3	2
v_r	12	12.5	14
v_{co}	25	20	25
R	16	29	46
Reference (Further Details)	[39]	[40]	[41]

3. Numerical Results and Discussion

3.1. Wind Turbines and Weibull Distribution Data

The models of the considered wind turbines are “GEV MP R”, G58-850, and E-92. The specifications of the WTs are given in Table 1 and their fit parameters are shown in Table 3. It is noteworthy that since polynomials are of a high order, we need to keep too many significant digits than we usually do in engineering practice (otherwise, the accuracy of the polynomial fit deteriorates).

Table 2. Scale and Shape Parameters of Weibull Distribution for Four Different Sites [2]; [4]

Location	Scale Parameter (c)	Shape Parameter (k)
Calabria, Italy	5.8	1.2
Ras Moneef, Jordan	7.25	2.39
Pyhatunturi, Finland	11.5	2
Thumrait, Oman	6.67	3.34

Fig. 3 shows WTPSC curve fits for E-92 WT. We observe that the 9th high-order polynomial fit accurately matches the manufacturer data for the GCR, while the approximate cubic fit tends to be shifted upwards. The exponential fit has quasi-linear characteristics with some of its WTPSC curve (in the GCR) being above the manufacturer data and some other being below. As for the PDF, Table 2 shows the values of the Weibull scale and shape parameters for four different sites. The parameters range from relatively small to relatively large values because we do not want to lose the generality.

3.2. Calculation Procedure

The calculation procedure used to obtain the results is described as follows

1. Apply regression analysis to obtain the coefficients in Table 3. This is done by collecting numerical data from databases in [39]–[41] for the GCR then using the Curve Fitting Toolbox in MATLAB.

Table 3. WTs Fit Parameters

Fit Type	WT Model		
	GEV MP R	G58-850	E-92
Polynomial (Eq. (6))	$c_7 = -9.7222222, c_6 = 531.8519$	$c_8 = -1.300386, c_7 = 85.39326$	$c_9 = -0.05359899, c_8 = 2.795792$
	$c_5 = -12209.44, c_4 = 152177.3$	$c_6 = -2365.413, c_5 = 36007.81$	$c_7 = -53.10329, c_6 = 364.1766$
	$c_3 = -1110157, c_2 = 4736572$	$c_4 = -328979, c_3 = 1845734$	$c_5 = 1508.517, c_4 = -41640.15$
	$c_1 = -10927270, c_0 = 10502880$	$c_2 = -6194947, c_1 = 11372350$	$c_3 = 290406, c_2 = -972119.1$
Approximate Cubic (Eq. (7))	$C_{p,max} = 0.3926$	$c_0 = -8744148$	$c_1 = 1609073, c_0 = -1048662$
	$K_p = 2.687, \beta = 2.201$	$C_{p,max} = 0.4453$	$C_{p,max} = 0.4729$
Exponential (Eq. (8))		$K_p = 12.88, \beta = 1.532$	$K_p = 11.12, \beta = 1.564$

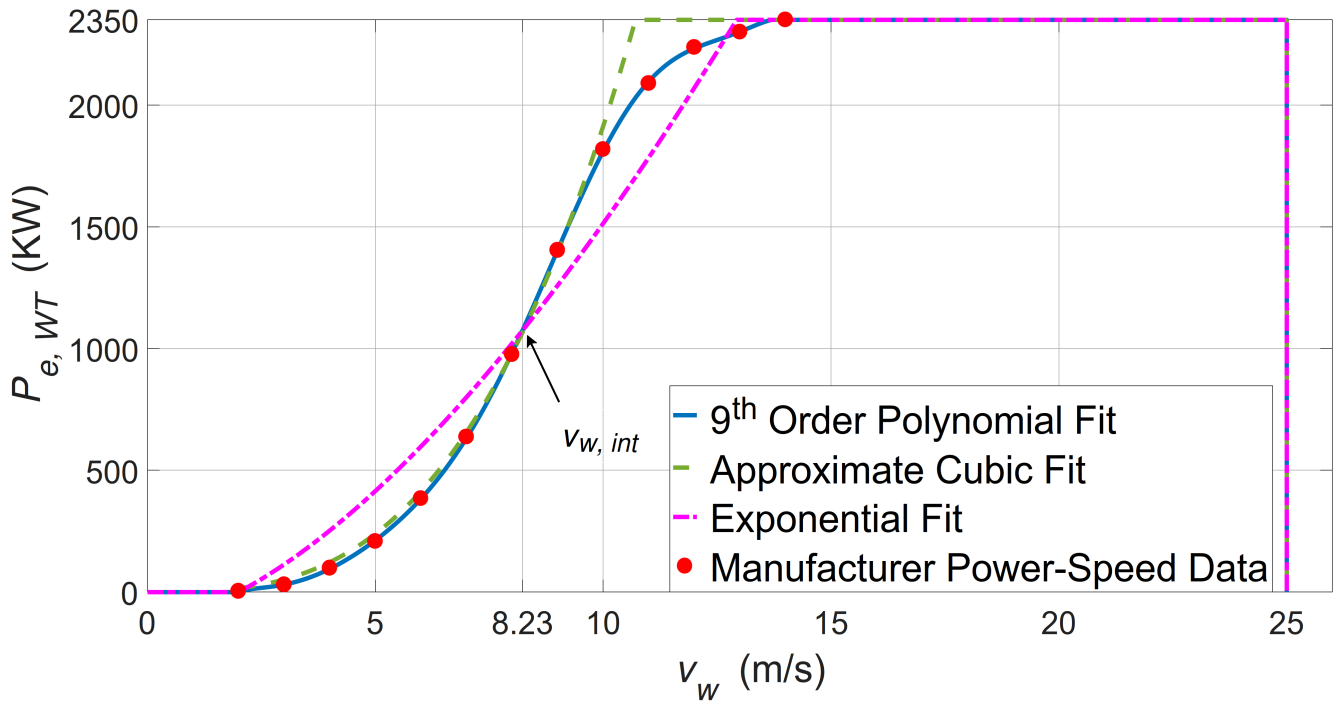


Fig. 3. WTPSC Curves with Different Fits for the GCR power-speed Pairs Provided by the Manufacturer (E-92)

- For polynomial and exponential models, the parameters of Eq. (6) are fit using linear regression. However, for exponential fit, the parameters of Eq. (7) are fit using nonlinear regression. Finally, for approximate cubic, the only parameter we must estimate is $C_{p, max}$ which is the maximum possible value for $C_{p, e}$ estimated using Eq. (3). Such step enables us to estimate $P_{e, WT}$ as given by Eq. (5)
2. Calculate $v_{w, int}$ in Fig. 3 which is simply the point at which WTPSC curve fits intersect. Using Eq. (11), estimate different average wind power outputs $\bar{P}_{e, WT}(0, \infty)$, $\bar{P}_{e, WT}(0, v_{w, int})$, and $\bar{P}_{e, WT}(v_{w, int}, \infty)$
 3. Apply Eq. (13) to calculate the capacity factor. Using polynomial fit as a reference, calculate the MSE and the percent errors. Repeat the steps above for all locations

3.3. Results and Discussion

Tables 4 and 5 show numerical results for C_f (in percent) of the combination of four different sites and the three WTs. From both tables, we note that the approximate cubic fit tends to overestimate C_f , which is attributed to the fact that it assumes a fixed value of power coefficient for all speeds which is equal to its maximum value for the given turbine (i.e., $C_{p, e} = C_{p, max}$ for all v_w in the GCR). Such an assumption would ultimately shift the power-speed curve upwards, causing the model to predict more energy yield, hence a higher C_f . For the approximate cubic fit, the maximum error in capacity factor calculations happens for the Ras Moneef area in Jordan with a value of roughly 5.1% when considering the E-92 WT. For G58-850 WT, the maximum error is 3.57%, which also corresponds to Ras Moneef in Jordan.

The exponential fit, however, tends to overestimate or underestimate C_f , which can be explained by the fact that

exponential fits may (in the GCR) have either larger or smaller power predictions than polynomial fit (see Fig. 3). Hence, we cannot make a general statement as to whether the error is positive or negative. For the exponential fit, the maximum absolute error in C_f calculations happens for Ras Moneef, Jordan, with a value of roughly 8.45% when considering the E-92 turbine. For G58-850 turbine, the maximum error is 3.9%, which also corresponds to Ras Moneef in Jordan. However, even though C_f is somewhat similar in these models, this would not mean that they are generally good. In this paper, we calculate $\bar{P}_{e, WT}(0, \infty)$, for E-92 WT using exponential model. Table 6 shows the results. We observe that the approximate cubic fit has some significant positive errors.

We can make a more thorough evaluation comparing the results of the exponential fit with those of the approximate cubic one. The exponential fit predicts higher power at lesser wind speeds and lower power at greater wind speeds, while the approximate cubic fit predicts higher power at all speeds. This is illustrated in Fig. 3. Hence, we may need to know how accurate is the exponential model in very windy and very calm days. Note from the curves in Fig. 3 that the exponential model intersects with the polynomial one at $v_{w, int} = 8.23$. After this speed, the former exhibits lesser power predictions, and before that speed, it exhibits greater power predictions.

Table 7 shows the $\bar{P}_{e, WT}(v_{w, int}, \infty)$, (for most of that range, the exponential model predicts greater wind power) values for the considered sites. Clearly, there are considerable downward (negative) errors from the average wind power as calculated by the polynomial fit. Such observation confirms that exponential models would predict significantly less power output in windy days. Looking at Table 8 (which is given for $\bar{P}_{e, WT}(0, v_{w, int})$) would let us draw different conclusions; the exponential fit here predicts much greater mean produced power for the low wind speed range, which is

the opposite of what we have just observed for the case of windy days. This, however, applies to “S-shaped” WT curves. Some WTs have quasi-linear characteristics in the GCR, which makes the exponential fit right to represent their GCR mathematically. This is what we elaborate on now.

By applying similar analysis on a WT with a quasi-linear curve in the GCR (model “GEV MP R”), we can tell that the exponential fit performs better than the approximate cubic fit in such case. We see this from C_f calculations in Table 9, where the approximate cubic fit has a maximum error of 6.1% corresponding to Thumrait in Oman, while the exponential fit

has a maximum error of 2.2%, which corresponds to Thumrait. The difference between the MSE resulting from exponential model and approximate cubic one confirms such claims.

Next, we evaluate the results of calculating the mean produced power. The results of using the approximate fit to calculate $\bar{P}_{e,WT}(0, \infty)$ for the considered sites are shown in Table 10. They have similar errors to the ones in Table 6 (which is for the same fit type). The maximum error, however, moderately increases (to 5.92%).

Table 4. C_f as Calculated Using Different Fits for WT Model E-92

	Calabria	Ras Moneef	Pyhatunturi	Thumrait	MSE
Polynomial	23.7	29.6	58.3	32.5	-
Approximate Cubic	24.8	31.1	60.1	33.8	2.1
Exponential	25.5	32.1	58.1	35.1	4.07

Table 5. C_f as Calculated Using Different Fits for WT Model G58-850

	Calabria	Ras Moneef	Pyhatunturi	Thumrait	MSE
Polynomial	23.7	30.8	57	34	-
Approximate Cubic	24.5	31.9	58.2	35.1	1.13
Exponential	24.2	32	56.5	35.3	0.908

Table 6. $\bar{P}_{e,WT}(0, \infty)$ Using Exponential Fit for WT Model E-92

	Calabria	Ras Moneef	Pyhatunturi	Thumrait
Polynomial	556	695	1371	764
Exponential	582	730	1413	798
Percent Error	4.67	5.04	3.06	4.45

Table 7. $\bar{P}_{e,WT}(v_{w,int}, \infty)$ using Exponential Fit for WT Model E-92

	Calabria	Ras Moneef	Pyhatunturi	Thumrait
Polynomial	421	448	1227	454
Exponential	394	402	1166	403
Percent Error	-6.4	-10.3	-4.97	-11.2

Table 8. $\bar{P}_{e,WT}(0, v_{w,int})$ using Exponential Fit for WT Model E-92

	Calabria	Ras Moneef	Pyhatunturi	Thumrait
Polynomial	135	247	144	310
Exponential	207	352	199	421
Percent Error	53.3	42.5	38.2	35.8

Table 9. C_f as Calculated Using Different Fits for WT Model “GEV MP R”

	Calabria	Ras Moneef	Pyhatunturi	Thumrait	MSE
Polynomial	21.5	25.8	56	27.9	-
Approximate Cubic	22.5	27.3	57.1	29.6	1.84
Exponential	21.6	26.2	55.9	28.5	0.135

Table 10. $\bar{P}_{e,WT}(0, v_{w,int})$ using Exponential Fit for WT Model “GEV MP R”

	Calabria	Ras Moneef	Pyhatunturi	Thumrait
Polynomial	59.2	71	154	76.8
Exponential	61.8	75.2	157	81.3
Percent Error	4.4	5.92	1.95	5.86

Table 11. $\bar{P}_{e,WT}(v_{w,int}, \infty)$ using Exponential Fit for WT Model “GEV MP R”

	Calabria	Ras Moneef	Pyhatunturi	Thumrait
Polynomial	46.4	46.2	138.8	44.4
Exponential	45.7	45.1	137.3	43.2
Percent Error	1.51	2.38	1.08	2.7

The results of using the exponential fit to calculate $\bar{P}_{e,WT}(v_{w,int}, \infty)$ (where $v_{w,int} = 8.48$) for the considered sites are shown in Table 11. We see significant improvements in the error with a maximum positive value of 2.7% compared to minimum negative value of 11.2% (Table 7). Such improvement is attributed to the quasi-linear characteristics of “GEV MP R” WT model in the GCR, which can be represented fairly well with the exponential fit (compared to the “S-shaped” characteristics of the E-92 in the GCR which cannot be represented well with the same fit).

We also use the exponential fit to calculate $\bar{P}_{e,WT}(0, v_{w,int})$ and their results are shown in Table 12. Significant improvements in the error can be seen. Here, we have maximum positive value of 8.47% compared to 53.3% (Table 8), which we, again, attribute the quasi-linear characteristics of “GEV MP R” WT model (the same reason mentioned above).

4. Conclusions

This paper examines the modeling of WTs and fitting its shape to the one provided by the manufacturer. We present evaluations in this paper for four different sites and three WTs of different ratings. We use the capacity factor, and the mean produced power for comparison purposes.

The exponential model may be quite inaccurate, especially when the WT has an “S-shaped” curve in the GCR and when considering low speeds. Such observation leads us to an important conclusion: when the exponential model tends to deviate from the manufacturer-provided data in the GCR, we may not accept the deviation even if some tend to be above and some below these data. This is because we may sometimes have fairly accurate prediction of the overall yield

(Table 4 and 5), but the accuracy when considering high and low speeds independently tends to greatly suffer (Table 7 and 8). In other words, positive and negative errors would offset each other when we consider the overall yield, but for very windy and very calm days, the predictions tend to suffer greatly. The approximate cubic model, however, seems to perform fairly well except for some inaccuracy when the WT has a quasi-linear curve in the GCR (Table 10).

Finally, it is evident that high-order polynomial fit the data very well, but getting a very high order (such as 9th or 8th) does not necessarily lead to an accurate representation of the GCR, but may rather result in an inaccurate representation at low wind speed near the cut-in speed of the WT.

References

- [1] G. Prakash and H. Anuta, “Future of wind - deployment, investment, technology, grid integration and socio-economic aspects,” IRENA, Tech. Rep., Oct. 2019.
- [2] H. Benbouhenni, “Application of five-level npc inverter in dpc-ann of doubly fed induction generator for wind power generation systems,” International Journal of Smart Grid, vol. 3, no. 3, pp. 128–137, 2019.
- [3] R. Ghajar, R. Chedid, and M. Badawieh, “Wind turbine optimal site matching based on capacity and availability factors,” in 2015 International Conference on Clean Electrical Power (ICCEP), Jun. 2015, pp. 253–257. DOI: 10.1109/ICCEP.2015.7177632.
- [4] Z. Shu, Q. Li, and P. Chan, “Statistical analysis of wind characteristics and wind energy potential in Hong Kong,” Energy Conversion and Management, vol. 101, pp. 644–657, 2015.

- [5] H. D. Ammari, S. S. Al-Rwashdeh, and M. I. Al- Najideen, "Evaluation of wind energy potential and electricity generation at five locations in Jordan," *Sustainable Cities and Society*, vol. 15, pp. 135–143, 2015.
- [6] S. Afanasyeva, J. Saari, M. Kalkofen, J. Partanen, and O. Pyrhönen, "Technical, economic and uncertainty modelling of a wind farm project," *Energy Conversion and Management*, vol. 107, pp. 22–33, 2016.
- [7] D. Astolfi, F. Castellani, and L. Terzi, "Wind turbine power curve upgrades," *Energies*, vol. 11, no. 5, p. 1300, 2018.
- [8] B. Manobel, F. Sehnke, J. A. Lazzús, I. Salfate, M. Felder, and S. Montecinos, "Wind turbine power curve modeling based on gaussian processes and artificial neural networks," *Renewable Energy*, vol. 125, pp. 1015– 1020, 2018.
- [9] J. Yan, H. Zhang, Y. Liu, S. Han, and L. Li, "Uncertainty estimation for wind energy conversion by probabilistic wind turbine power curve modelling," *Applied energy*, vol. 239, pp. 1356–1370, 2019.
- [10] B. Dongre and R. K. Pateriya, "Power curve model classification to estimate wind turbine power output," *Wind Engineering*, vol. 43, no. 3, pp. 213–224, 2019.
- [11] Y. Wang, Q. Hu, L. Li, A. M. Foley, and D. Srinivasan, "Approaches to wind power curve modeling: A review and discussion," *Renewable and Sustainable Energy Reviews*, vol. 116, p. 109 422, 2019.
- [12] R. Wadhvani and S. Shukla, "Analysis of parametric and non-parametric regression techniques to model the wind turbine power curve," *Wind Engineering*, vol. 43, no. 3, pp. 225–232, 2019.
- [13] N. Masseran, "Evaluating wind power density models and their statistical properties," *Energy*, vol. 84, pp. 533–541, 2015.
- [14] J. Tian, D. Zhou, C. Su, M. Soltani, Z. Chen, and F. Blaabjerg, "Wind turbine power curve design for optimal power generation in wind farms considering wake effect," *Energies*, vol. 10, no. 3, p. 395, 2017.
- [15] A. Harrouz, I. Colak, and K. Kayisli, "Energy modeling output of wind system based on wind speed," in 2019 8th International Conference on Renewable Energy Research and Applications (ICRERA), IEEE, 2019, pp. 63–68.
- [16] V. Katinas, M. Marčiukaitis, G. Gecevičius, and A. Markevičius, "Statistical analysis of wind characteristics based on weibull methods for estimation of power generation in lithuania," *Renewable energy*, vol. 113, pp. 190–201, 2017.
- [17] M. H. Ali, *Wind energy systems: solutions for power quality and stabilization*. CRC Press, 2012.
- [18] E. L. C. Arrieta, C. Cardona-Mancilla, J. Slayton, F. Romero, E. Torres, S. Agudelo, J. J. Arbelaez, and D. Hincapié, "Experimental investigations and cfd simulations of the blade section pitch angle effect on the performance of a horizontal-axis hydrokinetic turbine," *Engineering Journal*, vol. 22, no. 5, pp. 141–154, 2018.
- [19] H. M. S. M. Mazarbhuiya, A. Biswas, and K. K. Sharma, "Low wind speed aerodynamics of asymmetric blade h-darrieus wind turbine-its desired blade pitch for performance improvement in the built environment," *Journal of the Brazilian Society of Mechanical Sciences and Engineering*, vol. 42, no. 326, p. 326, 2020.
- [20] M. Allouche, S. Abderrahim, H. B. Zina, and M. Chaabane, "A novel fuzzy control strategy for maximum power point tracking of wind energy conversion system," *International Journal of Smart Grid*, vol. 3, no. 3, pp. 120–127, 2019.
- [21] J. Bukala, K. Damaziak, K. Kroszczyński, M. Krzeszowiec, and J. Malachowski, "Investigation of parameters influencing the efficiency of small wind turbines," *Journal of Wind Engineering and Industrial Aerodynamics*, vol. 146, pp. 29–38, 2015.
- [22] B. Wu, Y. Lang, N. Zargari, and S. Kouro, *Power conversion and control of wind energy systems*. John Wiley & Sons, 2011.
- [23] L. Saihi, Y. Bakou, A. Harrouz, I. Colak, K. Kayisli, and R. Bayindir, "A comparative study between robust control sliding mode and backstepping of a dfig integrated to wind power system," in 2019 7th International Conference on Smart Grid (icSmartGrid), IEEE, 2019, pp. 137–143.
- [24] J. D. De Kooning, T. L. Vandoorn, J. Van de Vyver, B. Meersman, and L. Vandevelde, "Displacement of the maximum power point caused by losses in wind turbine systems," *Renewable energy*, vol. 85, pp. 273– 280, 2016.
- [25] G. Bai, B. Fleck, and M. J. Zuo, "A stochastic power curve for wind turbines with reduced variability using conditional copula," *Wind Energy*, vol. 19, no. 8, pp. 1519–1534, 2016.
- [26] M. Lydia, S. S. Kumar, A. I. Selvakumar, and G. E. P. Kumar, "A comprehensive review on wind turbine power curve modeling techniques," *Renewable and Sustainable Energy Reviews*, vol. 30, pp. 452–460, 2014.
- [27] C. Carrillo, A. O. Montaña, J. Cidrás, and E. Díaz-Dorado, "Review of power curve modelling for wind turbines," *Renewable and Sustainable Energy Reviews*, vol. 21, pp. 572–581, 2013.
- [28] J. Chen, F. Wang, and K. A. Stelson, "A mathematical approach to minimizing the cost of energy for large utility wind turbines," *Applied energy*, vol. 228, pp. 1413– 1422, 2018.
- [29] R. J. de Andrade Vieira, M. A. Sanz-Bobi, and S. Kato, "Wind turbine condition assessment based on changes observed in its power curve," in 2013 International Conference on Renewable Energy Research and Applications (ICRERA), IEEE, 2013, pp. 31–36.
- [30] N. Masseran, "Evaluating wind power density models and their statistical properties," *Energy*, vol. 84, pp. 533–541, 2015.
- [31] I. Tizgui, F. El Guezar, H. Bouzahir, and B. Benaïd, "Comparison of methods in estimating weibull parameters for

wind energy applications,” *International Journal of Energy Sector Management*, vol. 11, no. 4, pp. 650–663, 2017.

[32] S. A. Akdağ and A. Dinler, “A new method to estimate Weibull parameters for wind energy applications,” *Energy conversion and management*, vol. 50, no. 7, pp. 1761–1766, 2009.

[33] T.-H. Yeh and L. Wang, “A study on generator capacity for wind turbines under various tower heights and rated wind speeds using Weibull distribution,” *IEEE Transactions on Energy Conversion*, vol. 23, no. 2, pp. 592–602, 2008.

[34] A.-R. Andrés and G. Osorio-Gómez, “Wind turbine selection method based on the statistical analysis of nominal specifications for estimating the cost of energy,” *Applied Energy*, vol. 228, pp. 980–998, 2018.

[35] Z. O. Olaofe and K. A. Folly, “Statistical analysis of the wind resources at darling for energy production,” *International Journal of Renewable Energy Research*, vol. 2, 2012.

[36] S. O. Ani, H. Polinder, and J. A. Ferreira, “Comparison of Energy Yield of Small Wind Turbines in Low Wind Speed Areas,” *IEEE Transactions on Sustainable Energy*, vol. 4, no. 1, pp. 42–49, Jan. 2013, ISSN: 1949-3029. DOI: 10.1109/TSTE.2012.2197426.

[37] S. Lindenberg, “20% Wind Energy by 2030 Increasing Wind Energy’s Contribution to U.S. Electricity Supply,” NREL, Tech. Rep., Jul. 2008.

[38] C. Moné, A. Smith, B. Maples, and M. Hand, “2013 Cost of Wind Energy Review,” NREL, Tech. Rep., Feb. 2015.

[39] [Online]. Available: <https://en.wind-turbine-models.com/turbines/436-vergnet-gev-mp-r-275-32> (Last Accessed 30/06/2020).

[40] [Online]. Available: <https://en.wind-turbine-models.com/turbines/762-gamesa-g58> (Last Accessed 30/06/2020).

[41] [Online]. Available: <https://en.wind-turbine-models.com/turbines/131-enercon-e-92> (Last Accessed 30/06/2020).